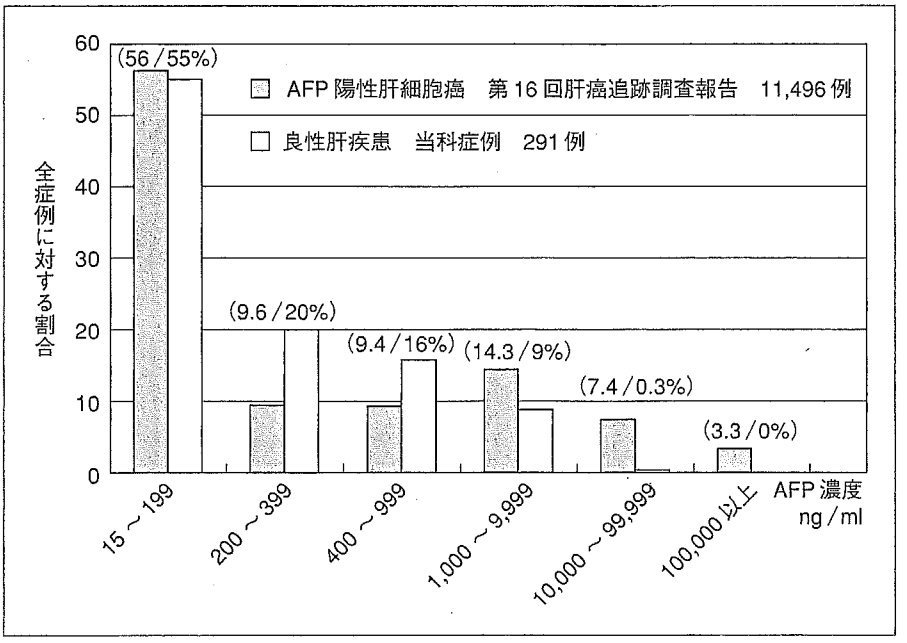

図1　良性肝疾患ならびにHCCにおけるAFP上昇の分布比較
第16回全国原発性肝癌追跡調査報告でAFP 15 ng/ml以上を示した11,496例のHCCのAFP濃度分布と当科におけるHCCを否定し得た良性肝疾患291例の分布の両者を示す．

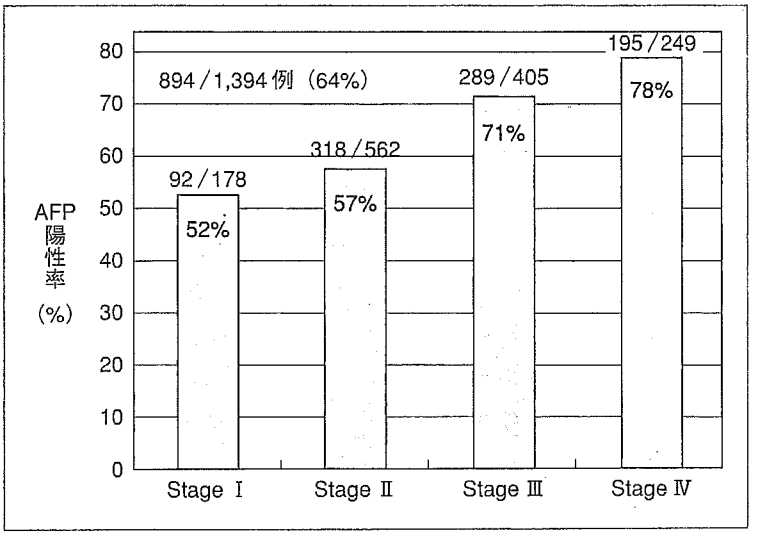

図2　当科でのHCCのStage別AFP陽性率

慢性肝疾患においてもしばしばその軽度な上昇を認める．当科の検討では，肝硬変(LC)で25%，慢性肝炎で17%が陽性を示している．図1に当科におけるHCCを否定した慢性肝疾患，主にLCでのAFP上昇を合わせて示すが，55%が200 ng/ml未満に分布している．第16回肝癌追跡調査報告での200 ng/ml未満のレンジにAFP陽性HCCの半数以上が分布するという結果を考え合わせると，良性肝疾患との鑑別が単回の濃度測定では極めて困難であることを示している．図3Aは500 ng/mlを上限として，当科でのHCCならびにLC，慢性肝炎，急性肝炎のAFP濃度をプロットしたものである．濃度でのHCCならびに良性肝疾患の識別は極めて困難であることが理解できる．

6．AFPの経時的推移

一般に，腫瘍の進展増大に伴いAFP濃度が上昇し，良性肝疾患との鑑別や治療効果判定の指標として用いることができる．しかしながら，早期のHCCにおいては，自然腫瘍壊死に伴い，無治

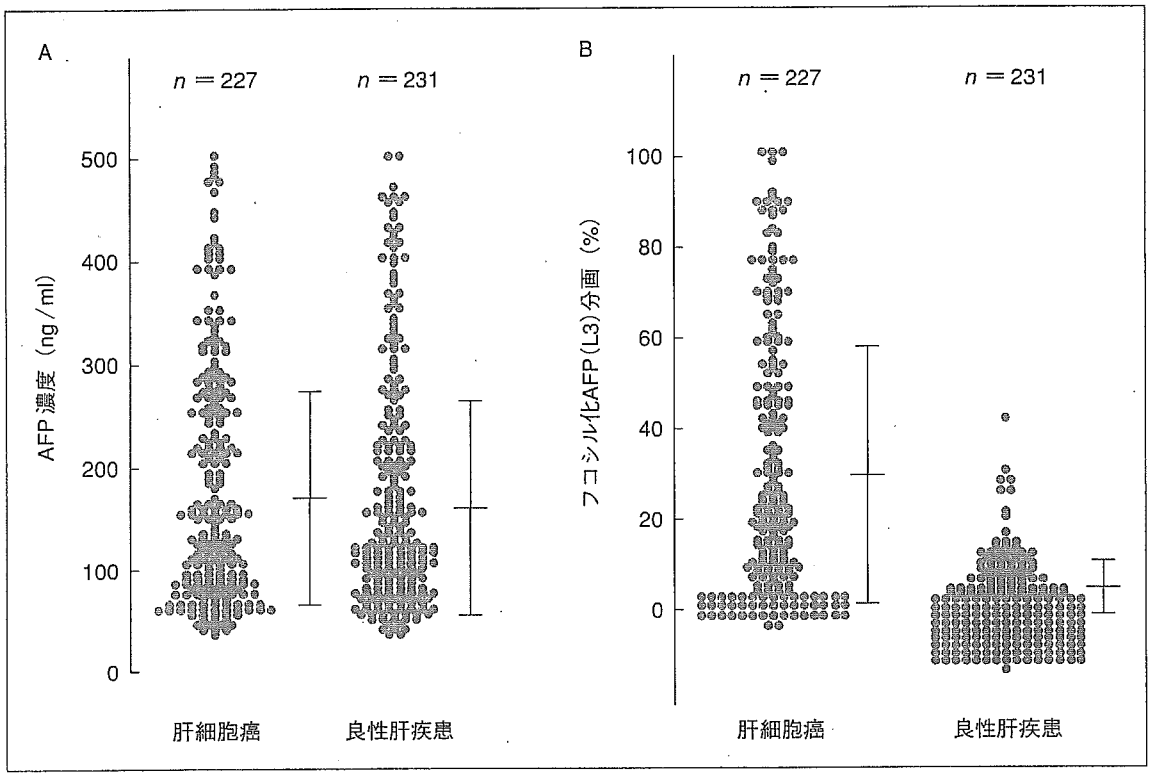

図3　HCC と良性肝疾患における AFP 濃度と L 3 分画のプロット
A：HCC 診断時の AFP 値が 500 ng/ml 以下の HCC 症例 227 例と同じく AFP 500 ng/ml 以下の良性肝疾患 231 例の血清 AFP 値のプロット．単なる AFP の絶対量では両疾患の鑑別は困難であることを示している．B：同症例での L 3 分画プロットで，両疾患の鑑別が可能であることを示す．

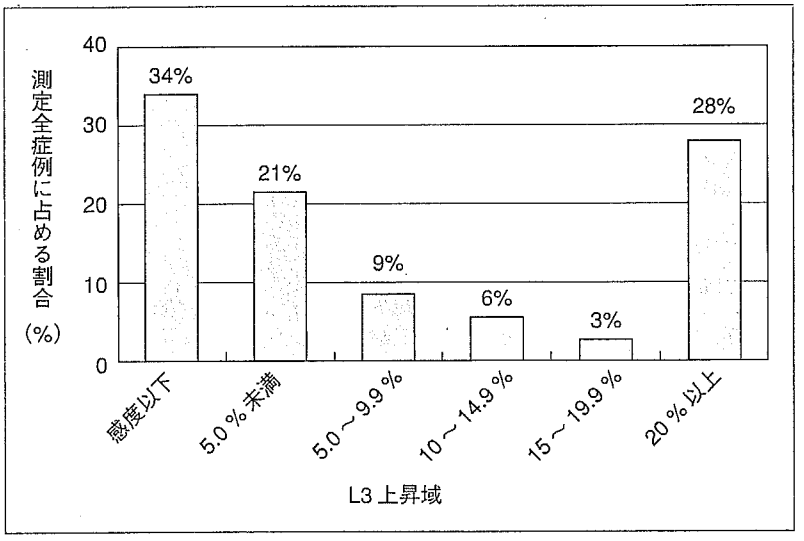

図4　16 回全国原発性肝癌追跡調査報告(2000～2001 の全国集計)での L 3 分画計測症例の結果

療にもかかわらず低下を示すことがある．すなわち，自然低下が必ずしも腫瘍の存在を否定することには結びつかない点に注意すべきである[2]．

L 3(フコシル化 AFP)分画による鑑別

1．癌化における AFP 糖鎖のフコシル化

筆者らは AFP の疾患特異性の向上を目的とした，HCC ならびに良性肝疾患由来 AFP の分子

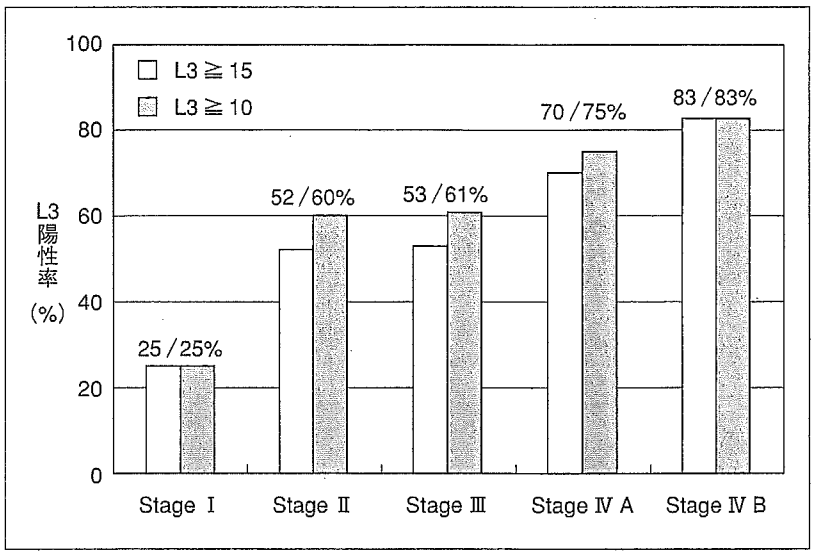

図5　当科におけるL3を計測し得たAFP産生HCC 298例でのStage別L3陽性率

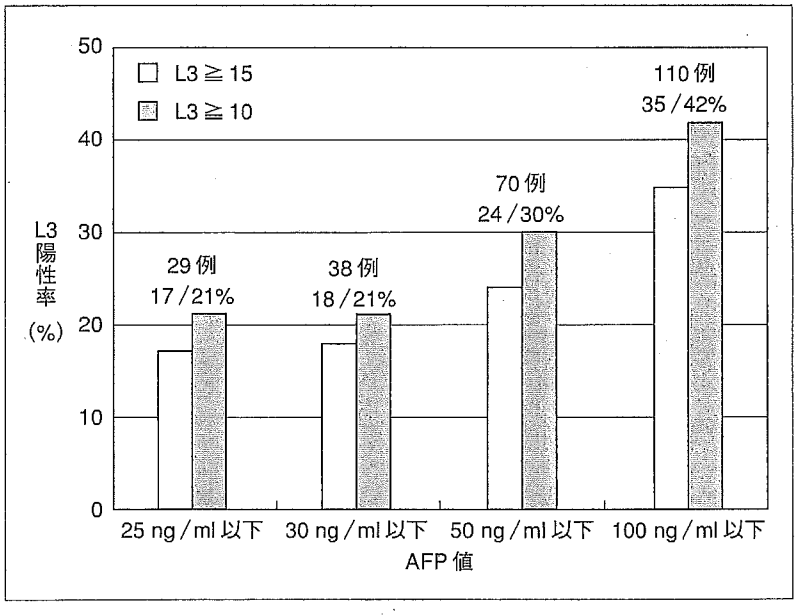

図6　当科におけるAFP低HCC症値例(25～100 ng/ml)でのL3陽性率

識別を行ってきた．そして，HCC由来AFPでは，良性肝疾患由来AFPに比較してレンズマメレクチンに親和性を有する分画の増加を認め[3]，この分画のAFPは二分岐複合型糖鎖の還元末端側の*N*-アセチルグルコサミンにα1-6のフコースが結合していることを見出した[4,5]．そして，総AFPに対するレンズマメレクチン結合性，すなわちフコシル化AFP分画のHCC早期診断における意義を報告してきた[2,6,7]．このフコシル化AFP分画はL3分画として保険収載されている[8]．

2．L3分画によるAFPの特異性向上

図3BはAFP濃度では重複しているHCC診断時のAFP値が500 ng/ml以下の症例と良性肝疾患症例のL3(フコシル化AFP)分画をプロットしたものである．同症例でのL3分画の平均は，HCC，良性肝疾患で，それぞれ30±29，4±7%(mean±SD)で，有意なHCC群での上昇を認めた．すなわち，AFP濃度では困難な両疾患の鑑別が可能であることを示している．また，

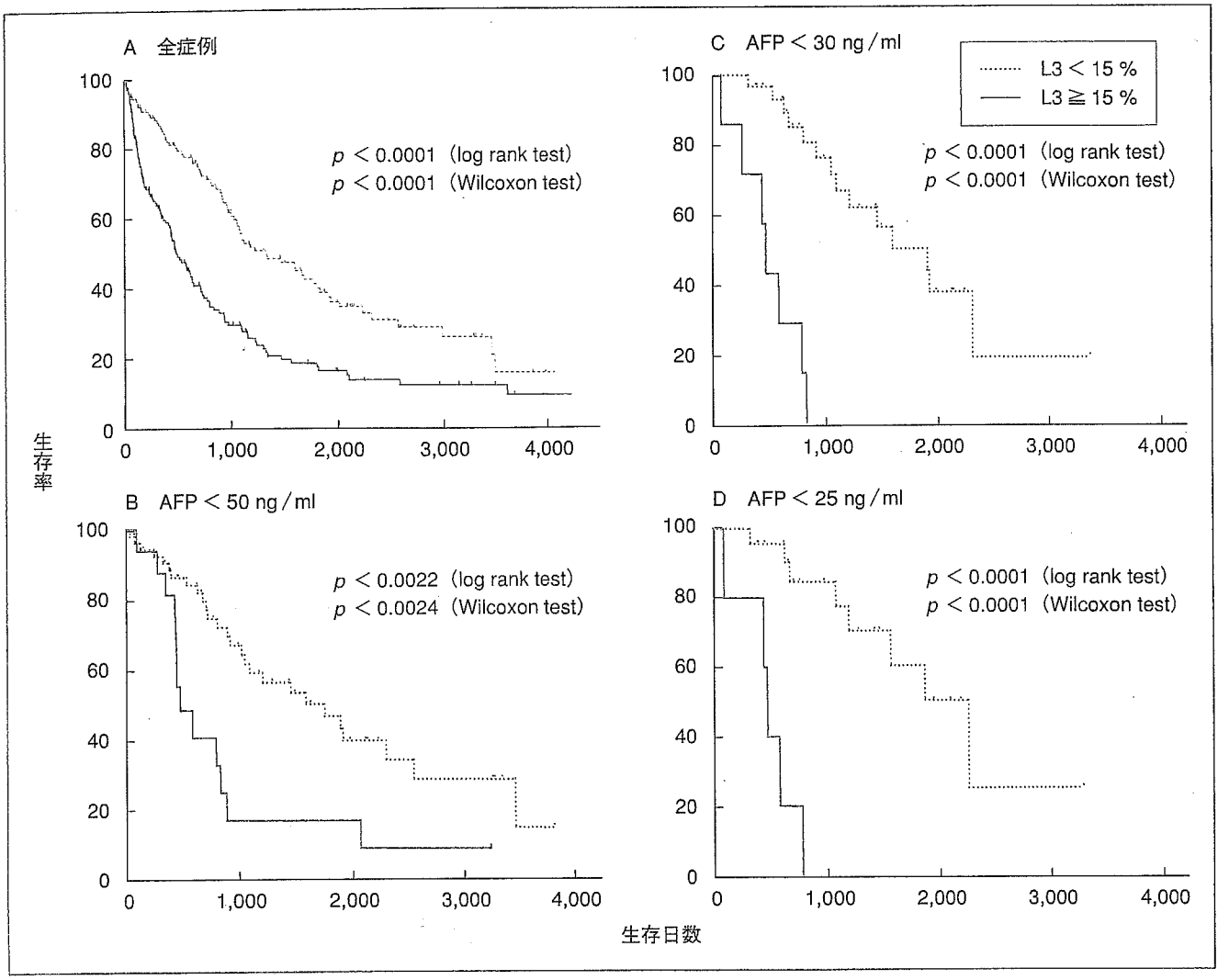

図7 L3分画高値，低値HCC群の生存率の比較
A：全症例(299例)での検討．B：AFP濃度が50 ng/ml以下の70例，C：30 ng/ml以下の38例，D：AFP濃度が25 ng/ml以下の29例での結果．

AFP濃度とL3は弱い相関関係を認めるのみで，互いに独立した因子としてみなすべきと考えられる[2]．

3．L3のカットオフ値

L3のカットオフ値としては10%とされているが，特異性を重用視しする場合は15%としたほうが望ましいと考えられる．

4．L3の診断能

第16回肝癌追跡調査報告の結果では，AFP濃度が17,538例に測定されているのに対して，L3分画が測定されているのは5,094例で全HCC例の29%にとどまっており，早期の普及が望まれる．この報告の結果を図4に示すが，L3のカットオフを10%とすると陽性率は37%，カットオフを15%とすると，陽性率は31%となる．この陽性率が低い理由として，最近のHCCが早期に診断されていることが予想されるが，Stage等のデータが公開されていないため詳細は不明である．当科でのL3分画の診断能を検討すると(15%をカットオフ)，陽性率(sensitivity)65%，LC，慢性肝炎を対照とした特異性(specificity)は96%で正診率(total accuracy)は74%であった[7]．

5．Stage別L3陽性率

当科でのL3を計測し得たHCC 298例での進行度別陽性率を図5に示す．Stage Iでは25%と低い値を示しているが，Stage II～IIIでは50～60%，Stage IVでは70～80%の陽性率を示している．この陽性率が高いという結果は，対象となるHCCとしてL3を計測するためにはAFP産生性であるというバイアスがかかっていることを

考慮する必要があるが，AFP陽性の場合には計測するに値する腫瘍マーカーであると考えられる．

6．AFP低値例での検討

図6はAFP値25～100 ng/mlでのHCC症例のL3陽性率を示す．カットオフ値にも関連するが，一般に非特異な上昇とされている数10 ng/ml程度の上昇レンジにおいてもその診断的価値が十分有ることを示している．このことは，後述する生物学的悪性度の指標としての臨床的意義についても同様である．

7．L3分画解釈上の注意点

LCなどにおける本分画の上昇(15%以上)はHCCが存在することを前提に各種画像診断を行う必要がある．また，10%を越えた症例も注意深く経過観察する必要がある．また，重要なことは，低値がすなわちHCCの否定にはつながらないことに留意すべきである．当科のデータではHCCの約30%で本分画が10%以下を示している．良性肝疾患でフコシル化分画20%以上を示した例は劇症肝炎を含む重症型急性肝炎または慢性肝炎の急性増悪や活動性LCの例が多く，臨床的に鑑別可能例が大半であった[7]．

生物学的悪性度の指標としてのL3分画

L3分画はHCCならびに良性肝疾患の鑑別以外にも，その生物学的悪性度を表すマーカーとしての意義が明らかになってきた[9,10]．図7Aは当科で治療後経過観察を行ったHCC 299例での検討を示す．診断時のL3分画のカットオフを15%とすると，高値群で，低値群に比較し有意な生存率の低下を認めている．また，この生存率の低下は，腫瘍進展度(Tumor stage)とは関係がなかった．そして，この傾向はAFP濃度が50～25 ng/mlと極めて低い症例においても認められた(図7B～D)．

治療目標としてのL3分画の解釈

HCC治療前後におけるL3分画を比較すると，治療後の経過観察例で本分画が低下した群では低下しなかった群に比較して良好な予後を示している[11]．すなわち，L3分画は肝癌細胞に特異性が高い分子種であることより，本分画が残っている限り十分な治療でないことを理解して治療に当たる必要があることを示している．

おわりに

腫瘍マーカーは各種悪性腫瘍の早期診断ならびに再発における意義のみならず，最近では予後規定因子や生物学的悪性度を評価する意義が次第に明らかになってきた[12]．今後，これらの新しい腫瘍マーカーの意義を含めた読み方がいっそう重要になると考えられる．

文　献

1）第16回全国原発性肝癌追跡調査報告，日本肝癌研究会，肝癌追跡調査委員会，進行印刷出版，2004
2）Aoyagi Y, Suzuki Y, Isemura M, et al：The fucosylation index of alpha-fetoprotein and its usefulness in the early diagnosis of hepatocellular carcinoma. Cancer 61：769-774, 1988
3）Aoyagi Y, Suzuki Y, Isemura M, et al：Differential reactivity of alpha-fetoprotein with lectins and evaluation of its usefulness in the diagnosis of hepatocellular carcinoma. Gann 75：809-815, 1984
4）Aoyagi Y, Isemura M, Yosizawa Z, et al：Fucosylation of serum alpha-fetoprotein in patient with primary hepatocellular carcinoma. Biochim Biophys Acta 830：217-223, 1985
5）Aoyagi Y, Suzuki Y, Igarashi K, et al：Carbohydrate structures of human alpha-fetoprotein of patients with hepatocellular carcinoma：Presence of fucosylated and non-fucosylated triantennary glycans. Br J Cancer 67：486-492, 1993
6）Aoyagi Y, Isemura M, Suzuki Y, et al：Fucosylated alpha-fetoprotein as marker of early hepatocellular carcinoma. Lancet ii：1353-1354, 1985
7）Aoyagi Y：Carbohydrate-based measurement on alpha-fetoprotein in the early diagnosis of hepatocellular carcinoma. Mini-Review. Glycocon J 12：194-199, 1995
8）Taketa K, Ichikawa E, Taga H, et al：Antiboby-affinity blotting, a sensitive technique for the detection of alpha-fetoprotein separated by lectin affinity electrophoresis in agarose gels. Electrophoresis 6：492-497, 1985
9）Yamashita F, Tanaka M, Satomura S, et al：Prognostic significance of *Lens culinaris* agglutinin A-reactive alpha-fetoprotein in small

hepatocellular carcinomas. Gastroenterology 111：996-1001, 1996
10) Aoyagi Y, Isokawa O, Suda T, et al：Fucosylation index of alpha-fetoprotein as a possible prognostic indicator in patients with hepatocellular carcinoma. Cancer 83：2076-2082, 1998
11) Aoyagi Y, Mita Y, Suda T, et al：The fucosylation index of serum a-fetoprotein as useful prognostic factor in patients with hepatocellular carcinoma. in special reference to chronological changes. Hepatolgy Res 23：287-295, 2002
12) 石井裕正，澤武紀雄，青柳豊，他：腫瘍マーカー，その診断的意義と今後の展開(座談会記録)，日本医師会雑誌 131：591-606, 2004

Journal of Medical Virology 78:44–52 (2006)

Tracing the History of Hepatitis B Virus Genotype D in Western Japan

Kojiro Michitaka,[1,2] Yasuhito Tanaka,[3] Norio Horiike,[1] Tran Nhu Duong,[1] Yan Chen,[1] Kana Matsuura,[1] Yoichi Hiasa,[1] Masashi Mizokami,[3] and Morikazu Onji[1]*

[1]*Third Department of Internal Medicine, Ehime University School of Medicine, Ehime, Japan*
[2]*Endoscopy Center, Ehime University School of Medicine, Ehime, Japan*
[3]*Department of Clinical Molecular Informative Medicine, Nagoya City University Graduate School of Medical Sciences, Nagoya, Japan*

The major hepatitis B virus (HBV) genotypes in Japan are B and C. HBV genotype D (HBV/D), however, is widespread in a small area of Western Japan, where the Gianotti–Crosti syndrome caused by HBV subtype *ayw*, which is suspected to be HBV/D, was endemic in the 1970s. The aim of the study was to elucidate its origin, time of transmission, and spread in this area. Genotyping of HBV-DNA was done in 363 patients with HBV infection. The year of birth was checked in patients with HBV/D. The full genome sequences of 20 HBV/D strains, 2 of which were obtained from a single carrier with a 19-year-interval, were analyzed. An evolutionary rate, the date of the most recent common ancestor, and the effective number of HBV/D infections were calculated. Fifty-two of 363 patients were infected with HBV/D, and 39 were born in 1970s. In a phylogenetic tree, the 20 HBV/D strains produced a definite cluster, and the evolutionary rate was calculated to be 5.4×10^{-5} nucleotide substitutions/site/year. The root of the tree was estimated to be in approximately 1,900 and began to spread from the 1940s, leading to a rapid increase of infected patients in the 1970s. From these results, it is suspected that HBV/D was likely transmitted to the area investigated approximately 100 years ago and then spread widely in the 1970s. From the history of the area and the genetic analysis, HBV/D in this area was speculated to be of Russian origin. ***J. Med. Virol. 78:44–52, 2006.***

KEY WORDS: hepatitis B surface antigen; subtype; evolutionary rate; complete genome sequence; Gianotti–Crosti syndrome; Japanese–Russian war

INTRODUCTION

Hepatitis B virus (HBV) is one of the major causes of liver disease throughout the world, as approximately 350 million people are infected chronically. HBV has approximately 3,200 bases that can be divided into several genotypes by sequence divergence, with 8 genotypes (A–H) reported [Okamoto et al., 1988; Norder et al., 1994; Stuyver et al., 2000; Arauz-Ruiz et al., 2002]. These genotypes have a distinct geographical distribution, with genotypes A (HBV/A) and HBV/D predominant in Europe, Middle East, Central Asia, Siberia, and America, HBV/B and HBV/C in East Asia, and HBV/E in Africa. In addition, HBV/F has been reported in Central America, and HBV/G in the United States and France [Norder et al., 1993; Lindh et al., 1997; Sanchez-Tapias et al., 2002; Chu et al., 2003; Miyakawa and Mizokami, 2003; Deversa et al., 2004; Mulders et al., 2004; Tallo et al., 2004]. In Japan, HBV/C is the most prevalent, followed by HBV/B, while others are encountered very rarely. Although the frequency of HBV/D was reported to comprise only 0.4% of HBV carriers in Japan [Orito et al., 2001], it was found recently that approximately 10% of the HBV carriers in a small geographical area (Ehime Prefecture) in Western Japan were infected with HBV/D [Duong et al., 2004]. In this area, an endemic occurrence of infantile

Institution at which the work was performed.

Grant sponsor: Ministry of Health, Labor, and Welfare of Japan.

*Correspondence to: Dr. Morikazu Onji, Ehime University School of Medicine, Shitsukawa, Toon-shi Ehime, 791-0295 Japan. E-mail: onjimori@m.ehime-u.ac.jp

Accepted 1 September 2005

DOI 10.1002/jmv.20502

Published online in Wiley InterScience (www.interscience.wiley.com)

papular acrodermatitis (Gianotti–Crosti syndrome), which is known to be related to acute HBV infection [De Gaspari et al., 1970; Gianotti, 1973], emerged in the 1970s, with the subtype (serotype) of the hepatitis B surface antigen (HBsAg) reported to be *ayw* in those patients, whereas that of the majority of other HBV carriers in this area are infected with subtype *adr* [Ishimaru et al., 1976; Toda et al., 1978]. Unfortunately, serum samples from those patients taken in 1970s are no longer available, although that of a girl with this syndrome taken in 1988 was kept and subsequent testing demonstrated that she was infected with HBV/D, serotype *ayw* [Michitaka et al., 2004]. Recently, it was reported that the deduced HBsAg serotype in all HBV/D strains studied in this area was *ayw3* [Duong et al., 2004], in contrast to the majority of HBV/C patients in Japan, who are known to be infected with serotype *adr*. From those results, it is speculated that HBV with subtype *ayw* found in patients with the Gianotti–Crosti syndrome from this area in 1970s was HBV/D, and the endemic occurrence of this disease was related to the spread of HBV/D in this area. Further, it is suspected that the HBV/D was not indigenous, but rather from abroad, since HBV/D is very rare in the surrounding districts.

In the present study, attempts were made to clarify the origin, time of transmission, and time of spread of HBV/D in this area using molecular evolutional analyzes.

MATERIALS AND METHODS

Patients

Three hundred and sixty-three patients (13–86 years old, median 45 years, 213 males and 150 females) with chronic HBV infection living in the Ehime Prefecture who attended hospital between 1997 and 2003 were examined for HBV genotypes and the year of birth. This was done to gain insight on the period of spread of genotype D. Among these patients, 253 patients had normal levels of serum aminotransferase (ALT) and 110 patients had elevated levels of ALT. Four of patients had a past history of Gianotti–Crosti syndrome. The purpose of the study was explained to patients before taking the samples and written informed consent was obtained from all patients.

Materials for Complete Genome Sequence

Twenty complete HBV genome sequences from 19 Japanese patients infected with HBV/D (8 women, 11 men, 13–86 years of age), 16 with chronic and 3 with acute infection, who were born and living in the Ehime Prefecture were analyzed. Among 16 patients with chronic infection, 14 had persistently normal ALT levels, whereas the other 2 had persistent or intermittent elevation of ALT levels. Two of the 20 HBV strains were from a single HBV carrier that was sampled with a 19-year-interval. Seven of the 20 HBV strains were reported previously, while the other 13 were newly sequenced for this study. The newly sequenced strains were selected at random from the patients in this study. Serum samples were stored at −80°C prior to genotyping and sequencing.

HBV Genotyping

The HBV genotype was determined based on the restriction fragment length polymorphism patterns of the *S* gene sequence following amplification by the polymerase chain reaction (PCR-RFLP) [Mizokami et al., 1999].

Complete Genome Sequence

Complete genome sequences were determined by direct sequencing of the PCR-products, the detail of which were described previously [Chen et al., 2003]. Briefly, DNA was extracted from sera and HBV-DNA was amplified by PCR. To obtain the full-length HBV-DNA sequence, 2 amplicons were obtained by PCR, and 1 fragment was 2,936 bases in length (nt 1,994–nt 1,747), and the other 1,080 bases in length (nt 1,399–nt 2,478). Sequencing was done by direct sequencing using a commercially available kit with suitable sequencing primers (BigDye Terminator Cycle Sequencing FS Ready Reaction Kit, Applied Biosystems, Alameda, CA). The accuracy of the sequence was ensured by identification of the sequence data of the complete genome obtained by sense sequencing primers and that obtained by anti-sense sequencing primers.

Estimating Evolutionary Rates and Dating the Origin of HBV

A reconstructed tree was produced using the concatenated non-overlapping regions of the HBV genome. Overlapping regions were excluded, because they are subject to complex evolutionary processes that might increase phylogenetic noise [Bollyky and Holmes, 1999; Fares and Holmes, 2002], resulting in a final alignment of 1,591 bases of the non-overlapping sequences for the phylogenetic analysis. The tree was built on the non-overlapping regions using a heuristic maximum-likelihood (ML) topology search with stepwise-addition and nearest neighbor-interchange algorithms. Tree likelihood scores were calculated using HKY85, with the molecular clock enforced using PAUP version 4.0b8. Using the estimated topology, all possible root positions were evaluated under a single rate dated tips (SRDT) model with the computer software TipDate v1.2 and the root that yielded the highest likelihood was adopted [Rambaut, 2000]. The program provided an ML estimate of the rate and also the associated date of the most recent common ancestor of the sequences, using a model that assumed a constant rate of nucleotide substitution. The molecular clock was tested by a likelihood ratio test between the SRDT model and a general unconstrained branch length model [different rate (DR) model]. To confirm the reliability of the phylogenetic tree, bootstrap resampling tests were also carried out 1,000 times.

Demographic Model

For estimates of demographic history, a non-parametric function N(t), also known as a skyline plot, was obtained by transforming the coalescent intervals of an observed genealogy into a piecewise plot that represented an effective population size through time [Pybus et al., 2001; Pybus and Rambaut, 2002]. A parametric ML was estimated by several models with the computer software Genie v3.0 to build a statistical framework for inferring the demographic history of a population on phylogenies reconstructed from sampled DNA sequences [Pybus and Rambaut, 2002]. This model assumes a continuous epidemic process in which the viral transmission parameters remain constant through time. Model fitting was evaluated by likelihood ratio tests of the parametric ML estimates [Lemey et al., 2003; Pybus et al., 2003]. Approximate 95% confidence intervals for the parameters were estimated using the likelihood ratio test statistics.

RESULTS

Year of Birth

The numbers of patients infected with HBV/A, HBV/B, HBV/C, and HBV/D were 6, 24, 281, and 52, respectively. Figure 1 shows the number of patients infected with HBV/C and HBV/ D in relation to years of birth. Patients with HBV/C were born within a wide spectrum of time (between 1940 and 1980). On the other hand, 39 of 52 patients infected with HBV/D were born in 1970s. All four patients who had a history of the Gianotti–Crosti syndrome were infected with HBV/D, and three were born in 1970s, whereas one was born in 1980s.

Complete Sequences of 20 HBV/D Strains

The 20 serum samples from 19 patients with HBV infection, whose HBV genotype was determined to be HBV/D by PCR-RFLP, were subjected to complete HBV genome sequencing. The accession numbers of the 20 complete HBV genome sequences and additional information regarding the infected patients are shown in Table I. All 20 strains were found to be 3,182 bases in length except 1 with 3,194 bases (AB090269), and the deduced HBsAg serotype was *ayw3* in all 20 strains. No recombinant sequences with other HBV genotypes were detected in any of these 20 HBV complete genomes. Among 19 patients, 1 patient whose HBV sequence was Ehime D5 had the history of sexual contact with 2 patients whose HBV were Ehime D3 and Ehime D4. Other 16 patients had no history of mutual contact.

Phylogenetic Relationship Among Ehime HBV Strains

An un-rooted ML tree for the non-overlapping regions of the HBV genome is represented in Figure 2. The 20 strains from Ehime, which were HBV/D, showed a significant cluster with a high bootstrap value, and some European and Russian (Kamchatka) strains, especially a Swedish strain (AY090453), were found to be closely related. Such a significant cluster is suitable for a coalescent analysis. As the tree topology on the non-overlapping regions was quite similar to that of the complete genomes, the tree on the non-overlapping

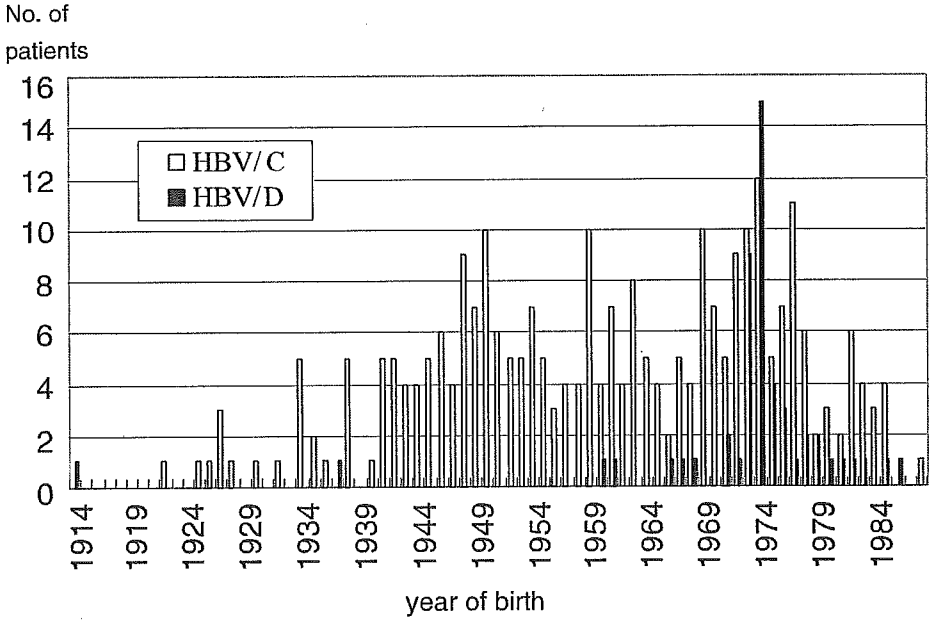

Fig. 1. The years of birth of patients infected with hepatitis B virus (HBV)/C and HBV/D. Numbers of patients infected with HBV/C was shown by white bars, whereas that with HBV/D was shown by black bars.

TABLE I. Hepatitis B Virus (HBV) Genotype D Sequences in Ehime Prefecture Used in This Study

Sequence	Accession no.	Length of genome (bp)	Serotype	Sex	Age	Date of collection	Aminotransferase (ALT)	HBeAg	Diagnosis[a]	Reference
Ehime D1	AB090268	3,182	*ayw3*	M	27	1997	88	+	CH	Duong et al. [2004]
Ehime D2	AB090269	3,194	*ayw3*	M	64	1992	39	+	CH	Duong et al. [2004]
Ehime D3	AB078031	3,182	*ayw3*	F	18	1998	7,620	+	FH	Chen et al. [2003]
Ehime D4	AB078032	3,182	*ayw3*	F	20	2000	189	+	AH	Chen et al. [2003]
Ehime D5	AB078033	3,182	*ayw3*	M	19	1998	42	+	ASC	Chen et al. [2003]
Ehime D6	AB090270	3,182	*ayw3*	M	21	1999	46	+	ASC	Duong et al. [2004]
Ehime D7	AB109475	3,182	*ayw3*	F	64	2001	33	+	ASC	Present study
Ehime D8	AB109476	3,182	*ayw3*	M	70	1997	21	+	ASC	Present study
Ehime D9	AB109477	3,182	*ayw3*	M	24	1997	21	+	ASC	Present study
Ehime D10	AB109478	3,182	*ayw3*	M	24	1998	14	−	ICS	Present study
Ehime D11	AB109479	3,182	*ayw3*	F	25	1997	15	−	ICS	Present study
Ehime D12	AB110075	3,182	*ayw3*	F	86	2001	11	−	ICS	Present study
Ehime D13	AB119251	3,182	*ayw3*	M	28	2002	40	−	ICS	Present study
Ehime D14	AB119252	3,182	*ayw3*	M	27	2002	24	−	ICS	Present study
Ehime D15	AB119253	3,182	*ayw3*	M	26	2000	43	−	ICS	Present study
Ehime D16	AB119254	3,182	*ayw3*	M	28	2003	26	−	ICS	Present study
Ehime D17	AB119255	3,182	*ayw3*	F	28	2001	12	−	ICS	Present study
Ehime D18	AB119256	3,182	*ayw3*	F	23	1997	21	−	ICS	Present study
Ehime D19	AB116266	3,182	*ayw3*	F	13	1987	1,452	−	AH	Michitaka et al. [2004]
Ehime D20	AB120308	3,182	*ayw3*	F	66	1982	378	+	AH	Present study

[a]AH, acute hepatitis; FH, fulminant hepatitis; CH, chronic hepatitis; ASC, asymptomatic HBV carrier; ICS, inactive hepatitis B surface antigen (HBsAg) carrier state [Lok and McMahon, 2001].
Isolates Ehime D12 and Ehime D20 are from the same patient.

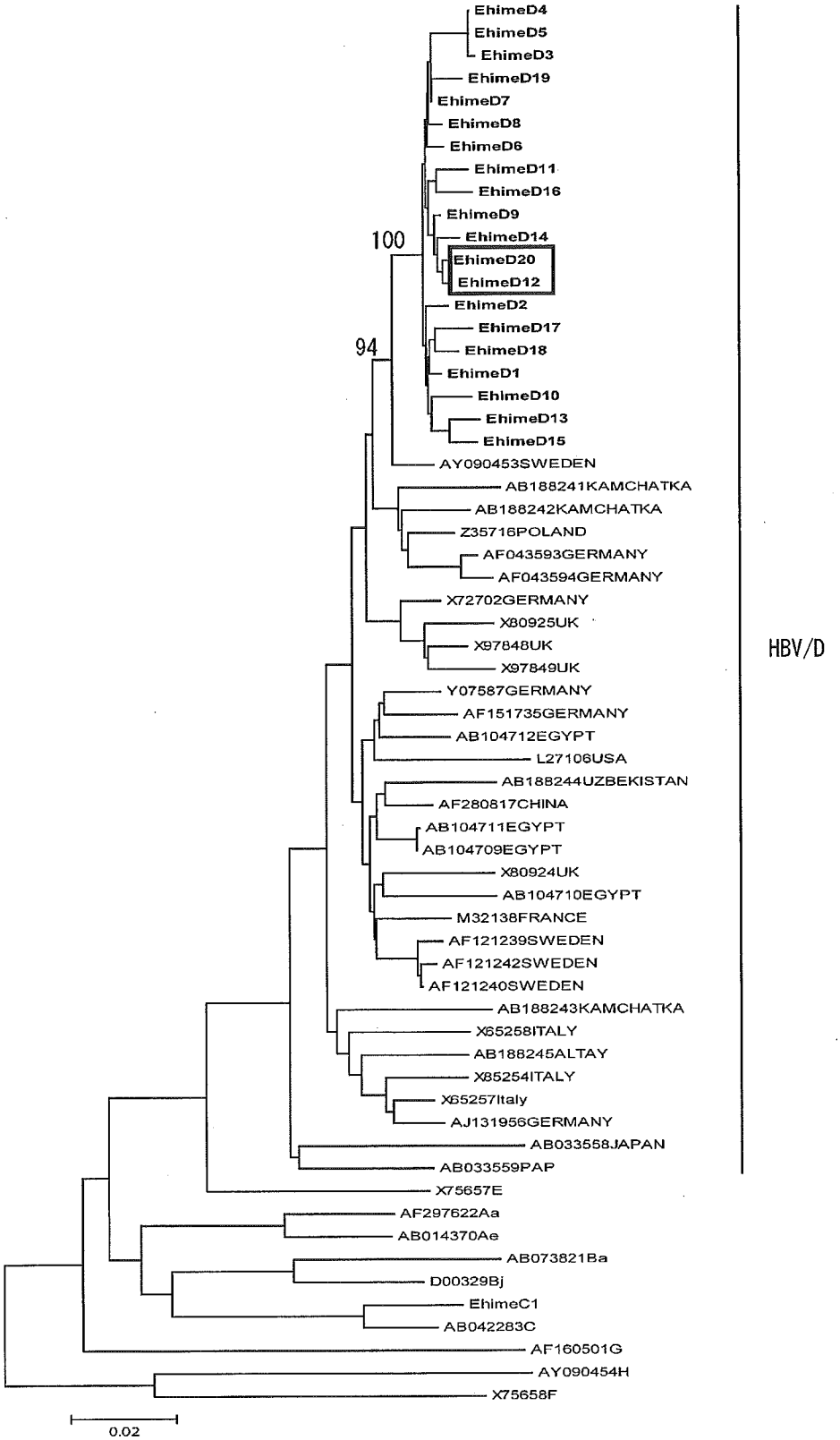

Fig. 2. A phylogenetic tree constructed using non-overlapping sequences of 20 HBV/D strains from Ehime and reference sequences. Reference isolates from the database are identified with accession number, and each country name was added in all HBV/D strains. The Ehime strains in this study were shown in bold. The number in the tree indicates bootstrap reliability. Isolates Ehime D12 and Ehime D20 are from the same patient surrounded by open square.

sequences was used in this study to exclude phylogenetic noise [Bollyky and Holmes, 1999; Fares and Holmes, 2002].

Rates and Demographic History of HBV Evolution

To determine the evolutionary rate of HBV, the 20 HBV/D strains, which included 2 strains (AB110075, AB120308) obtained from the same subject with a 19-year interval, were subjected to molecular evolutionary analyses. The molecular evolutionary rate was estimated by two independent methods. Briefly, direct comparison on non-overlapping sequences with a 19-year interval obtained from the same subject indicated that a molecular evolutionary rate was 5.9×10^{-5} nucleotide substitutions/site/year. Second, TipDate (v1.2) was used to compare the DR model with the single rate (SR) and SRDT models. The SR model was rejected ($P < 0.01$) and the SRDT model provides an adequate fit to the data ($P = 0.15$). Based on the SRDT model, the mean rate of nucleotide substitutions was estimated to be 5.4×10^{-5} nucleotide substitutions/site/year (95% confidence intervals of 4.0×10^{-5} to 7.2×10^{-5}), which was similar to the rate (4.2×10^{-5}) estimated by Fares and Holmes [2002], and resulted in a date estimate of 1902 for the root of the tree (95% confidence intervals of 1,867–1,927).

Based on the phylogenetic tree, the effective number of HBV infections through time, N(t), was analyzed using a skyline plot for the Ehime HBV strains. The parameters for several models in Genie v3.0 were also examined. Time t was then transformed to year using the same rate, assuming the collecting time to be the present. Figure 3 shows the skyline plots and population growth for the HBV patients in Ehime, according to a specific demographic model in Genie v3.0 with three parameters, a piecewise expansion growth model, which was evaluated by likelihood ratio testing [Lemey et al., 2003; Pybus et al., 2003]. Based on this molecular evolution, it was estimated that the divergence time of the most recent common ancestor of HBV/D in Ehime was also estimated to be approximately 1,900. Further, the Ehime HBV/D strains of Ehime began to increase in the 1940s, and the time of spread was estimated to be around 1970 when the spread time was defined temporally as 10% of the present population size of HBV infections (Fig. 3).

DISCUSSION

The HBV/D strains in Ehime were found to have a significant cluster with a high bootstrap value and were clearly distinct from most European strains. Such a significant cluster is suitable for a coalescent analysis. The specific demographic model based on the neutral theory [Pybus et al., 2001, 2003; Lemey et al., 2003], which has a constant size in the past and changes to exponential growth until the present, was applied for investigating the Japanese endemic of HBV/D in Ehime.

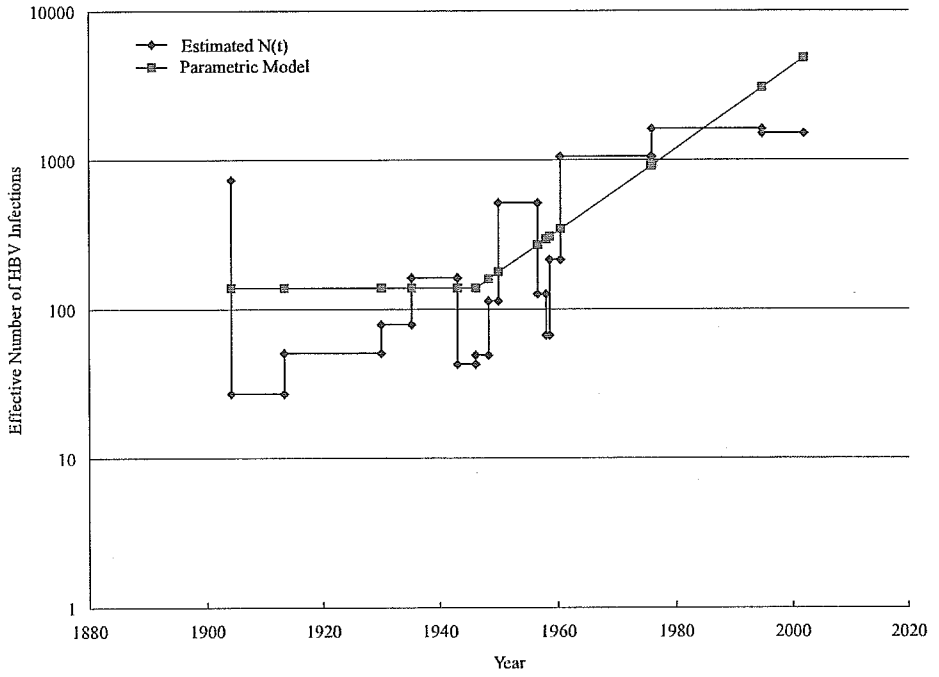

Fig. 3. The maximum-likelihood (ML) estimates of N(t) on the effective number of HBV/D infections in Ehime. The parametric model is indicated by the magenta line and stepwise plots by the blue line, which represent corresponding non-parametric estimates of N(t) (number as a function of time). Genetic distances have been transformed into a time scale of years using estimates of the molecular clock in non-overlapping regions of HBV.

Several historical factors in Japan have probably affected the spread of HBV/D, such as an increase of intravenous drug abuse in the 1940s during and after World War II, and the increase of blood transfusion procedures and the use of non-sterilized medical materials in the 1960s and 1970s. Using molecular evolutionary analyses; the spread of HBV/D in Ehime was determined to have started in the 1940s and rapidly increased around 1970. The endemic occurrence of the Gianotti–Crosti syndrome by HBV with serotype *ayw* in the investigated area emerged in 1970s [Ishimaru et al., 1976], which were close to the estimated spread time of HBV/D in the present study. Many infant patients with the Gianotti–Crosti syndrome in this region were reported to have progressed to a chronic carrier state [Toda et al., 1978]. The fact that majority of the patients infected with HBV/D were born in 1970s indicates a relationship with the endemic of this disease in infants in 1970s because the Gianotti–Crosti syndrome occurred at this time. It was not possible to ascertain the exact time of infection in individual cases, therefore, it is a limitation of this study. However, the time of birth was almost similar, and this circumstantial evidence strongly supports the calculated data from the molecular evolutionary analyses that the time of spread of the infection was 1970s. Although the infectious routes have not been clarified, the use of non-sterilized medical equipment such as injection needles in children may be one of the important routes. It is another problem whether HBV/D with serotype *ayw3* has a character to induce the Gianotti–Crosti syndrome, or whether HBV/D strains from patients with this syndrome have a peculiar motif in their nucleotide or amino acid sequences. This issue should be clarified in the future.

The molecular evolutionary analyses revealed that the time of the root of the HBV/D tree in this area was estimated to be around 1,900. It is of an interest to understand how HBV/D was transmitted to the Ehime area and where it originated from. The history of this region is likely important to solve this issue. Communication between people living in Ehime and those in foreign countries was not frequent prior to the end of the 19th century. However, in the period of time around 1900, Japan became involved in several wars, such as the Japanese–Sino War from 1894 to 1895, the Japanese–Russian War from 1904 to 1905, and World War I from 1914 to 1918. In connection with these international conflicts, many foreigners came to this area, since Matsuyama city in the Ehime Prefecture had a naval port and a large prison camp, in which approximately 100 Chinese prisoners of war were interned from 1894 to 1895, followed by 6,000 Russian prisoners from 1904 to 1906, and 500 German prisoners from 1914 to 1917. These incidents were considered to have played a role in the importation of HBV/D from other countries to this region of Japan. Among the wars noted above, the Japanese–Sino War is thought to have no relation with the spread of HBV/D, because the prevalence of HBV/D in China is very low [Miyakawa and Mizokami, 2003]. Based on the present data that the divergence time of the most recent common ancestor of HBV/D in Ehime to be approximately 1,900, the Japanese–Russian War is the most likely candidate as the initial event that led to HBV/D transmission in Japan.

Four subgenotypes (D1–D4) have been described for HBV/D [Norder et al., 2004]. The 20 isolates in the present study were assigned D2. Two isolates from Kamchatka in Russia shown in Figure 2 (AB188241, AB188242) were also assigned D2. The subtype of HBsAg of the 20 strains was *ayw3*. Several reports have described an association between drug abuse and infection with HBV subtype *ayw3*. van Steenbergen et al. [2002] performed a molecular epidemiological study of acute hepatitis B in Amsterdam, and found that HBV from majority of drug users were genotype D with subtype *ayw3*. Swenson et al. [2001] studied the HBV genotypes and HBsAg subtypes in refugees and injection drug users in the United States, and found that 7 of 15 refugees from former Soviet Union and 17 of 32 drug users were infected with HBV/D with subtype *ayw3*. Further, they described that HBsAg subtype of HBV/D strains from the majority of the drug users showed regular *ayw3* of which HBsAg had Thr 118 and Met 125, whereas that of the seven refugees from Soviet Union showed variant *ayw3* of which HBsAg had Val 118 or Ala 118 and Thr 125. All of the 20 strains in the present study had HBsAg with Val 118 and Thr 125, which was identical with variant *ayw3* of refugees from former Soviet Union in their study. Interestingly, the phylogenetic analysis indicated that the HBV/D strains with subtype *ayw3* in drug users and refugees from former Soviet Union formed a cluster along with the 20 strains in present study and some European strains from database (Fig. 4). Although this phylogenetic tree was not constructed with complete HBV genome, this result supports the speculation that the HBV/D in Ehime would be originated from Russia. As intravenous drug users had been common in 1940s in Japan, indeed, they might have played some role in the spread of HBV/D in this area.

The present study showed that HBV/D has been spreading rapidly in the intervening century. The infectious routes of blood transfusion, non-sterilized medical materials, and maternal transmission are well controlled now, however, sexual transmission, which is the most common infectious route for adults in Japan [Arima et al., 2003], remains uncontrolled. On the other hand, several reports from the metropolitan area in Japan have described that acute hepatitis with HBV/A infection due to sexual transmission has been increasing [Kobayashi et al., 2002; Ogawa et al., 2002]. Those reports together with the present study led to the suspicion that HBV/A and HBV/D, whose main infectious routes are horizontal, might become the dominant genotypes in Japan in the future, rather than HBV/B and HBV/C, whose main infectious route is vertical, if a suitable preventive policy for HBV transmission is not established. Thus, in order to control the spread of HBV, especially HBV/A and HBV/D, additional efforts are

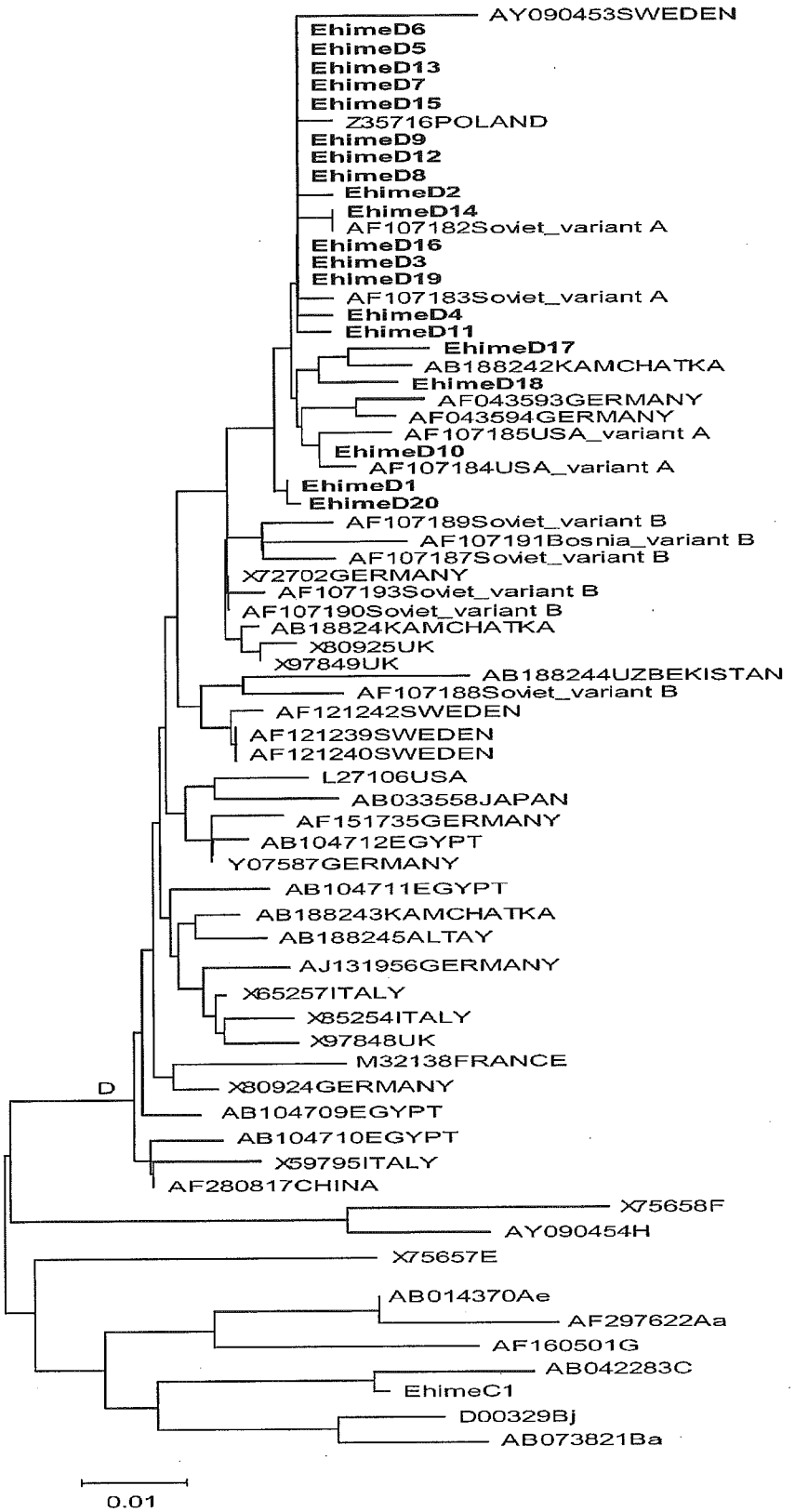

Fig. 4. A phylogenetic tree constructed using small *S* gene (nt 478–774) of 20 HBV/D strains from Ehime and reference sequences.

needed to prevent sexual transmission because universal vaccination against HBV has not yet been introduced in Japan.

In conclusion, HBV/D at the Ehime area in Japan showed a definite cluster, and molecular evolutionary analyses indicate that its root was likely to be around 1,900, followed by a rapid spread in the 1970s.

REFERENCES

Arauz-Ruiz P, Norder H, Robertson BH, Magnius LO. 2002. Genotype H: A new Amerindian genotype of hepatitis B virus revealed in Central America. J Gen Virol 83:2059–2073.

Arima S, Michitaka K, Horiike N, Kawai K, Matsubara H, Nakanishi S, Abe M, Hasebe A, Tokumoto Y, Yamamoto K, Onji M. 2003. Change of acute hepatitis B transmission routes in Japan. J Gastroenterol 38:772–775.

Bollyky PL, Holmes EC. 1999. Reconstructing the complex evolutionary history of hepatitis B virus. J Mol Evol 49:130–141.

Chen Y, Michitaka K, Matsubara H, Yamamoto K, Horiike N, Onji M. 2003. Complete genome sequence of hepatitis B virus (HBV) from a patient with fulminant hepatitis without precore and core promoter mutations: Comparison with HBV from a patient with acute hepatitis infected from the same infectious source. J Hepatol 38: 84–90.

Chu CJ, Keeffe EB, Han SH, Perrillo RP, Min AD, Soldevila-Pico C, Carey W, Brown RS, Jr., Luketic VA, Terrault N, Lok AS, the US HBV Epidemiology Study Group. 2003. Hepatitis B virus genotypes in the United States: Results of a nationwide study. Gastroenterology 125:444–451.

De Gaspari G, Bardare M, Costantino D. 1970. AU antigen in Crosti–Gianotti acrodermatitis. Lancet 1:1116–1117.

Deversa M, Rodriguez C, Leon G, Liprandi F, Pujol FH. 2004. Clade analysis and surface antigen polymorphism of hepatitis B virus American genotypes. J Med Virol 72:377–384.

Duong TN, Horiike N, Michitaka K, Yan C, Mizokami M, Tanaka Y, Jyoko K, Yamamoto K, Miyaoka H, Yamashita Y, Ohno N, Onji M. 2004. Comparison of genotypes C and D of the hepatitis B virus in Japan: A clinical and molecular biological study. J Med Virol 72: 551–557.

Fares MA, Holmes EC. 2002. A revised evolutionary history of hepatitis B virus (HBV). J Mol Evol 54:807–814.

Gianotti F. 1973. Papular acrodermatitis of childhood. An Australia antigen disease. Arch Dis Child 48:794–799.

Ishimaru Y, Ishimaru H, Toda G, Baba K, Mayumi M. 1976. An epidemic of infantile papular acrodermatitis (Gianotti's disease) in Japan associated with hepatitis-B surface antigen subtype ayw. Lancet 1:707–709.

Kobayashi M, Arase Y, Ikeda K, Tsubota A, Suzuki Y, Saito S, Kobayashi M, Suzuki F, Akuta N, Someya T, Matsuda M, Sato J, Takagi K, Miyakawa Y, Kumada H. 2002. Viral genotypes and response to interferon in patients with acute prolonged hepatitis B virus infection of adulthood in Japan. J Med Virol 68:522–528.

Lemey P, Pybus OG, Wang B, Saksena NK, Salemi M, Vandamme AM. 2003. Tracing the origin and history of the HIV-2 epidemic. Proc Natl Acad Sci USA 100:6588–6592.

Lindh M, Andersson AS, Gusdal A. 1997. Genotypes, nt 1858 variants, and geographic origin of hepatitis B virus—Large-scale analysis using a new genotyping method. J Infect Dis 175:1285–1293.

Lok AS, McMahon BJ, Practice Guidelines Committee, American Association for the Study of Liver Diseases. 2001. Chronic hepatitis B. Hepatology 34:1225–1241.

Michitaka K, Horiike N, Chen Y, Duong TN, Konishi I, Mashiba T, Tokumoto Y, Hiasa Y, Tanaka Y, Mizokami M, Onji M. 2004. Gianotti–Crosti syndrome caused by acute hepatitis B virus genotype D infection. Intern Med 43:696–699.

Miyakawa Y, Mizokami M. 2003. Classifying hepatitis B virus genotypes. Intervirology 46:329–338.

Mizokami M, Nakano T, Orito E, Tanaka Y, Sakugawa H, Mukaide M, Robertson BH. 1999. Hepatitis B virus genotype assignment using restriction fragment length polymorphism patterns. FEBS Lett 450:66–71.

Mulders MN, Venard V, Njayou M, Edorh AP, Bola Oyefolu AOB, Kehinde MO, Muyembe Tamfum JJM, Nebie YK, Maiga I, Ammerlaan WQ, Fack F, Omilabu SA, La Flaou A, Mullar CP. 2004. Low genetic diversity despite hyperendemicity of hepatitis B virus genotype E throughout West Africa. J Infect Dis 190:400–408.

Norder H, Hammas B, Lee SD, Bile K, Courouce AM, Mushahwar IK, Magnius LO. 1993. Genetic relatedness of hepatitis B viral strains of diverse geographical origin and natural variations in the primary structure of the surface antigen. J Gen Virol 74:1341–1348.

Norder H, Courouce AM, Magnius LO. 1994. Complete genomes, phylogenetic relatedness, and structural proteins of six strains of the hepatitis B virus, four of which represent two new genotypes. Virology 198:489–503.

Norder H, Courouce AM, Coursaget P, Echevarria JM, Lee SD, Mushahwar IK, Robertson BH, Locarnini S, Magnius LO. 2004. Genetic diversity of hepatitis B virus strains derived worldwide: Genotypes, subgenotypes, and HBsAg subtypes. Intervirology 47: 289–309.

Ogawa M, Hasegawa K, Naritomi T, Torii N, Hayashi N. 2002. Clinical features and viral sequences of various genotypes of hepatitis B virus compared among patients with acute hepatitis B. Hepatol Res 23:167–177.

Okamoto H, Tsuda F, Sakugawa H, Sastrosoewignjo RI, Imai M, Miyakawa Y, Mayumi M. 1988. Typing hepatitis B virus by homology in nucleotide sequence: Comparison of surface antigen subtypes. J Gen Virol 69:2575–2583.

Orito E, Ichida T, Sakugawa H, Sata M, Horiike N, Hino K, Okita K, Okanoue T, Iino S, Tanaka E, Suzuki K, Watanabe H, Hige S, Mizokami M. 2001. Geographic distribution of hepatitis B virus (HBV) genotype in patients with chronic HBV infection in Japan. Hepatology 34:590–594.

Pybus OG, Rambaut A. 2002. GENIE: Estimating demographic history from molecular phylogenies. Bioinformatics 18:1404–1405.

Pybus OG, Charleston MA, Gupta S, Rambaut A, Holmes EC, Harvey PH. 2001. The epidemic behavior of the hepatitis C virus. Science 292:2323–2325.

Pybus OG, Drummond AJ, Nakano T, Robertson BH, Rambaut A. 2003. The epidemiology and iatrogenic transmission of hepatitis C virus in Egypt: A Bayesian coalescent approach. Mol Biol Evol 20:381–387.

Rambaut A. 2000. Estimating the rate of molecular evolution: Incorporating non-contemporaneous sequences into maximum likelihood phylogenies. Bioinformatics 16:395–399.

Sanchez-Tapias JM, Costa J, Mas A, Bruguera M, Rodes J. 2002. Influence of hepatitis B virus genotype on the long-term outcome of chronic hepatitis B in Western patients. Gastroenterology 123: 1848–1856.

Stuyver L, De Gendt SL, Van Geyt C, Zoulim F, Fried M, Schinazi RF, Rossau R. 2000. A new genotype of hepatitis B virus: Complete genome and phylogenetic relatedness. J Gen Virol 81:67–74.

Swenson PD, Van Geyt C, Alexander ER, Hagan H, Freitag-Koontz JM, Wilson S, Norder H, Magnius LO, Stuyver L. 2001. Hepatitis B virus genotypes and HBsAg subtypes in refugees and injection drug users in the United States determined by LiPA and monoclonal EIA. J Med Virol 64:305–311.

Tallo T, Norder H, Tefanova V, Krispin T, Priimagi L, Mukomolov S, Mikhailov M, Magnius LO. 2004. Hepatitis B virus genotype D strains from Estonia share sequence similarity with strains from Siberia and may specify ayw4. J Med Virol 74:221–227.

Toda G, Ishimaru Y, Mayumi M, Oda T. 1978. Infantile papular acrodermatitis (Gianotti's disease) and intrafamilial occurrence of acute hepatitis B with jaundice: Age dependency of clinical manifestations of hepatitis B virus infection. J Infect Dis 138: 211–216.

van Steenbergen JE, Niesters HGM, Op de Coul ELM, van Doornum GJJ, Osterhaus ADME, Leetvaar-Kuijpers A, Coutinho RA, van den Hoek JAR. 2002. Molecular epidemiology of hepatitis B virus in Amsterdam 1992–1997. J Med Virol 66:159–165.

ELSEVIER

European Journal of Radiology 53 (2005) 312–317

EJR
EUROPEAN JOURNAL OF RADIOLOGY

www.elsevier.com/locate/ejrad

Abdominal virtual ultrasonographic images reconstructed by multi-detector row helical computed tomography

Masashi Hirooka, Hidehito Iuchi, Kiyotaka Kurose, Teru Kumagi, Norio Horiike, Morikazu Onji*

Third Department of Internal Medicine, Ehime University School of Medicine, Shigenobu-cho, Onsen-gun, Ehime 791-0295, Japan

Received 5 January 2004; received in revised form 12 March 2004; accepted 16 March 2004

Abstract

Background: Three-dimensional (3D) images can be generated using thin sections from multi-detector row computed tomography (CT) and computer software, simulating images obtained using conventional ultrasonography (US). This software allows easy diagnosis of abdominal lesions and subsequent treatment of focal liver lesions such as hepatocellular carcinoma (HCC). The present study used newly developed virtual US software for diagnose and treatment of hepatobiliary disease. *Methods:* The software was used to create virtual US images in 10 subjects. Radiofrequency ablation (RFA) was performed by virtual US in seven patients with HCC. *Results:* Slices were easily reconstructed from various angles, and each slice was continuously animated as with conventional US in all subjects. Moreover, when seven patients with HCC were examined using virtual US, HCC nodules were visualized and could be treated with RFA. *Conclusions:* Virtual US should prove useful for visualization of HCC nodules that cannot be seen under conventional US. Virtual US is a useful tool for US-guided treatment of HCC.

Keywords: Virtual ultrasonography; Multi-detector row CT; Abdomen

1. Introduction

Ultrasonography (US) allows the body to be scanned from various positions and angles; whereas, the images generated by conventional computed tomography (CT) are displayed as horizontal tomographic slices. This means that clinicians must synthesize mentally a three-dimensional (3D) model of the body from multiple two-dimensional (2D) horizontal CT images, creating the equivalent of an ultrasound image. At present, diagnosis of abdominal lesions and treatment of liver focal lesions such as hepatocellular carcinoma (HCC) are performed using 2D images from US. Mental reconstruction is the most important and difficult task in US. Multi-detector row CT (MDCT) [1,2] offers the ability to rapidly scan large longitudinal volumes, and can scan volumes over a large range within a short time with thin slice images. MDCT images are then used to reconstruct 3D images. After reconstruction, multiplanar reformat (MPR) images resemble conventional ultrasonographic images [3]. Using a computer system, slices are animated continuously, and the user immerses in and interacts with totally virtual images.

The software used for virtual US in the present study reconstructed images comparable to those from conventional US. Utilizing these virtual images, radiofrequency ablation (RFA) could be performed for HCC that could not be clearly visualized on conventional US.

2. Materials and methods

2.1. Patients

The present study included 10 subjects (nine males and one female). All were admitted to the Third Department of Internal Medicine at Ehime University School of Medicine. Informed consent was obtained from all subjects prior to US and CT. Mean age was 70.5 years (range, 45–89 years). Subjects comprised eight patients with HCC, one with pancreatic cancer, and one liver transplant donor. All patients with HCC displayed type C liver cirrhosis, and mean tumor diameter was 1.8 cm (range, 1.0–3.5 cm). All tumors were

* Corresponding author. Tel.: +81 89 960 5308; fax: +81 89 960 5310.
E-mail address: onjimori@m.ehime-u.ac.jp (M. Onji).

0720-048X/$ – see front matter
doi:10.1016/j.ejrad.2004.03.026

visualized on dynamic CT. RFA was performed in seven patients with HCC with surgical hepatectomy in the remaining patient. Patients undergoing RFA displayed incomplete necrotic area due to previous RFA treatment, and this was attributable to poor visualization of puncture site. The eight nodules were located in the anterior segment of the right lobe ($n = 5$), posterior segment of the right lobe ($n = 2$), and medial segment of the left lobe ($n = 1$). One 75-year-old man with pancreatic cancer displayed a lesion in the head of the pancreas. In order to estimate the relationship between the pancreas and other organs, virtual imaging was used. The donor for liver transplantation (a 45-year-old man) was studied preoperatively for further examination of relevant arterial and venous anatomy.

2.2. Ultrasonography

US was performed after overnight fasting. A US system (SSD-6500, Aloka, Tokyo, Japan) was used. Patients were placed in the supine position with shoulders, buttocks, and heels in contact with the table. Water-soluble transmission gel was applied to the 3.5 MHz transducer.

2.3. Computed tomography

CT was also performed after overnight fasting, with the patient in the supine position and using a CT scanner (LightSpeed Ultra 16, GE Medical Systems, Milwaukee, WI). Contrast medium (Iopamiron, Eisai, Tokyo, Japan) was injected intravenously. Scanning parameters were: 0.625 mm collimation × 16; table speed, 6 mm/s (pitch, 1.75); 350–400 mA; 120 kV; 512 × 512 matrix. Transverse images were reconstructed at 0.625 mm intervals with a 0.625 mm section overlap. All MDCT data were transferred to the 3D workstation described below.

2.4. Virtual ultrasonography

This system runs smoothly on a personal computer with 2.0 GHz dual CPU (Xeon, Intel, CA), 2.0 GB RAM, Quadro 4 900XGL graphics card and Windows 2000 operating system.

For synthesis of 3D images and generation of virtual US images, VirtualPlace Advance software (Medical Imaging Laboratory, Tokyo, Japan; http://www.milab.jp) was used (Fig. 1). MPR images were reconstructed using MDCT data [3], and slices were displayed in a fan shape to resemble conventional US. Using a computer system, slices are animated continuously, and the user immerses in and interacts with totally virtual images [4].

2.5. Clinical experience

Dynamic CT was performed first. Using these CT images, virtual US images were reconstructed. Scanning with a virtual US probe, lesions were described in virtual US images. Conventional US was then performed on patients. A conventional US probe was used in the same location that the virtual US probe had been used. Images made using conventional and virtual US were then compared, and efficacy of virtual US was evaluated.

2.6. Radiofrequency ablation

Virtual images were revisualized using conventional US, confirming that conventional and virtual US images were very similar. The puncture needle was visualized as a hyperechoic silhouette on the monitor, and the needle was advanced to the target site. The HCC nodule was poorly visualized on US due to the obstruction from the lung, and water was injected into the right pleural cavity to produce artificial pleural effusion (500 mL of 5% glucose). A 17-gauge Cool-Tip electrode with a 2 cm exposed metallic tip (Radionics, Burlington, MA) was introduced via the puncture needle to the target site. A 480 kHz monopolar radiofrequency generator was used.

3. Results

Figs. 1 and 2 are CT images from the donor for liver transplantation. Fig 1A shows a whole abdominal image reconstructed by volume rendering. In this 3D image, the virtual US probe and US beam are shown, and placement of the probe and angles of decline can be seen. Fig. 1B shows virtual US images. Fig. 1C–E show horizontal, sagittal, and coronal slices, respectively.

First, the whole abdominal area was scanned using virtual US. Reconstructing slices from various angles was not problematic, and each slice was continuously animated just as in conventional US (Fig. 2). By tilting the virtual probe from cranially to caudally (Fig. 2, lower row), the entire abdominal area could be scanned (Fig. 2, upper row).

Virtual US in a patient with pancreatic cancer invading the splenic vein (Fig. 3B) was followed by conventional US performed with reference to virtual images (Fig. 3A). The abdominal aorta and transverse colon were identified in the same position on both conventional and virtual US. In a patient with HCC in the posterior segment of the right lobe (Fig. 4), virtual US identified the tumor between the anterior and posterior–inferior branch of the portal vein. Imaging showed that the posterior–inferior branch was separated from the posterior–superior branch (Fig. 4A). Liver morphology and vascular arrangements indicated that conventional and virtual US (Fig. 4B) yielded identical results. Images from virtual US were clearer than those of conventional US. In cases involving poor visualization on conventional US, anatomical relationships were easily understood using virtual US.

In a representative case (75-year-old man with HCC) of RFA (Fig. 5A), the nodule was in the subphrenic area, so

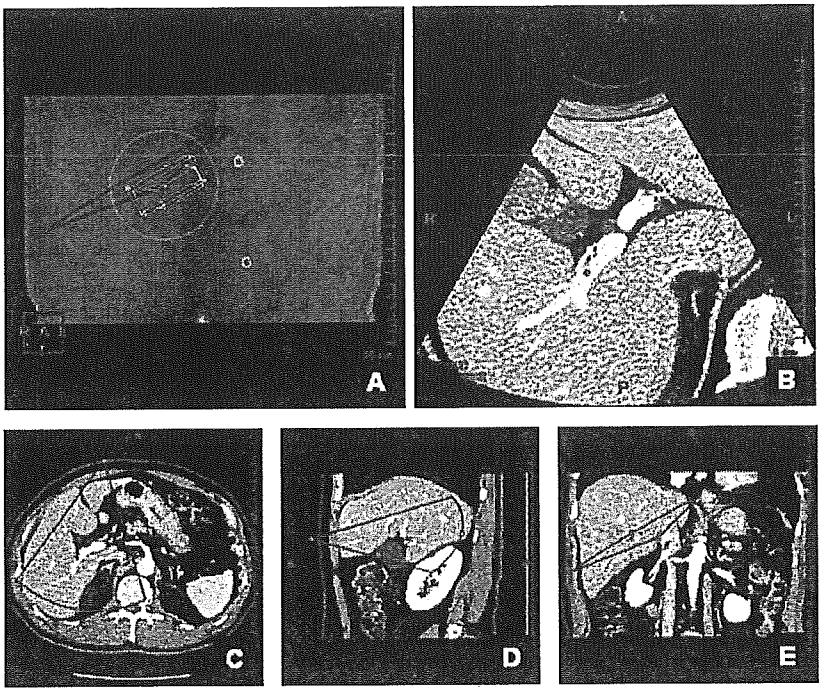

Fig. 1. The images made by the newly developed software. (A) Volume rendering image for whole abdomen. In this 3D image, the virtual US probe and US beam are shown. (B) Image from virtual US using virtual probe. (C–E) Horizontal, sagittal, and coronal sections, respectively, obtained by altering position of the virtual probe.

artificial pleural effusion was created before performing RFA. A gray point was placed in the area that had been treated incompletely using CT (Fig. 5B), then virtual images were reconstructed (Fig. 5C). The gray point was placed on the same site in virtual images (Fig. 5B and C). The virtual image was revisualized using conventional US, and puncture to the target area was performed (Fig. 5D). After treatment, dynamic CT revealed accurate ablation of the target site. Complete necrosis was also obtained by RFA in all seven patients with HCC. No severe complications occurred.

4. Discussion

The abdominal area is complex, and includes numerous organs and vessels that make understanding the structure of the abdomen difficult for sonographers. US allows slices across the whole abdominal area to be scanned from various positions and angles. Imagining abdominal structures based on 2D images from US is often difficult. However, using thin sections from CT and computer software, 3D images can be generated to accurately simulate those obtained using conventional US. The present study used virtual US software,

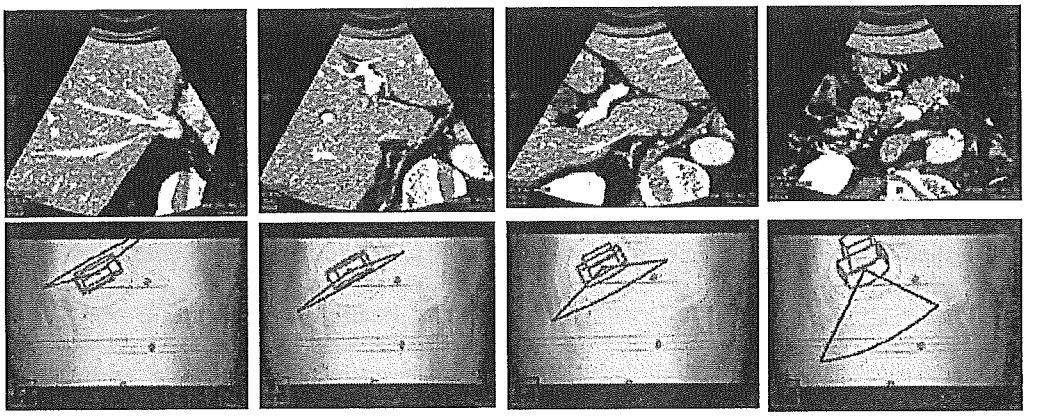

Fig. 2. Continuous scanning for virtual ultrasonography. Slices are reconstructed from various angles, with each slice continuously animated as in conventional US.

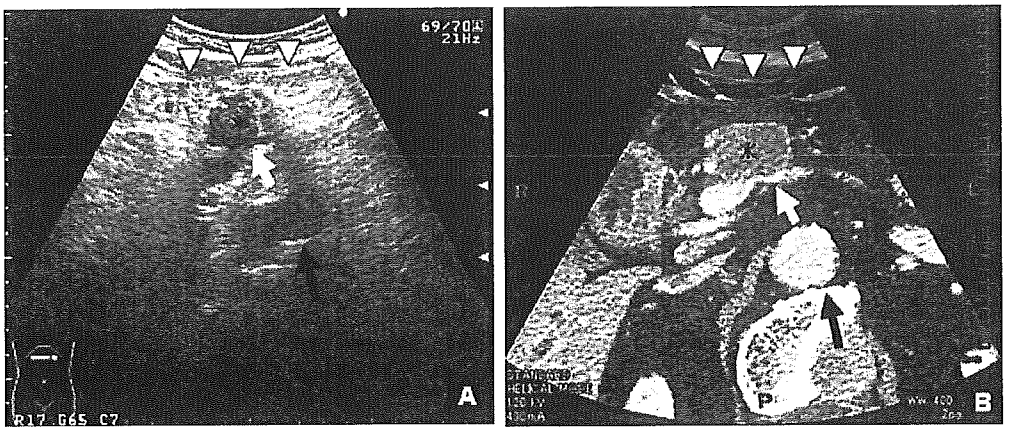

Fig. 3. A case of pancreatic cancer. (A) Conventional imaging from a patient with pancreatic cancer. Tumor is invading a splenic vein (white arrow). Transverse colon (white arrowhead) and abdominal aorta (black arrow) are shown. (B) Virtual imaging. Comparison of A and B confirms that virtual and conventional images depict the same anatomical structures and relationships.

and confirmed that images from virtual US are equal to and clearer than those from conventional US.

Significant changes have followed improvements in computer software and hardware resulting in new approaches to representing animation of diagnostic imaging. Use of virtual endoscopy has become widespread [5,6]. Scanning a virtual US probe from various angles and directions allows virtual US to be performed just like conventional US (Fig. 2). Virtual images can depict the peripheral vessels of the liver and closely resemble real images. Moreover, the organs and structures surrounding target lesions are represented in the same place, so users can readily grasp relationships between target lesions and other organs.

Virtual US has many clinical applications. First, virtual US provides an excellent educational tool for beginners. Various medical training systems based on multimedia and computer graphics have been reported [7,8], and requests for education and training in abdominal US are increasing. Using the present system, beginners can readily understand which organ is shown, and can practice identifying not only solid organs such as the liver, pancreas, and kidney, but also hollow organs like the stomach, colon, bile duct, and blood vessels. Moreover, various patterns and lesions can be demonstrated simply by changing the imaging data. Users can thus recreate abdominal anatomy in detail and utilize this knowledge when implementing the treatment.

Second, virtual US can be applied to treatment. Non-surgical treatment of HCC is typically performed using guidance from US [9–13]. However, comparing images from US and CT is often difficult [14]. Using the present software, agreement between US and CT images can be confirmed. Virtual US is also very useful for the treatment of nodules that cannot be visualized on US, but are apparent on CT. A nodule described by virtual US can readily be placed on conventional US using the surrounding anatomical relationships. Furthermore, virtual US is useful in RFA

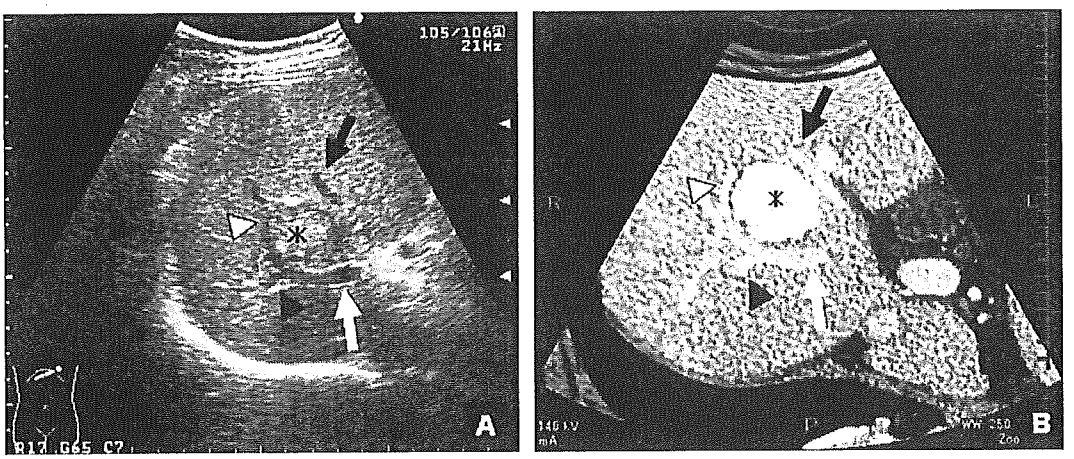

Fig. 4. A case of hepatocellular carcinoma. (A) Conventional US showing a nodule between the anterior branch (black arrow) and posterior–inferior branch (white arrow) of the portal vein (PV). The posterior–inferior branch (white arrowhead) is separated from the posterior–superior branch (black arrowhead). (B) Virtual US closely resembles the conventional US shown in (A).

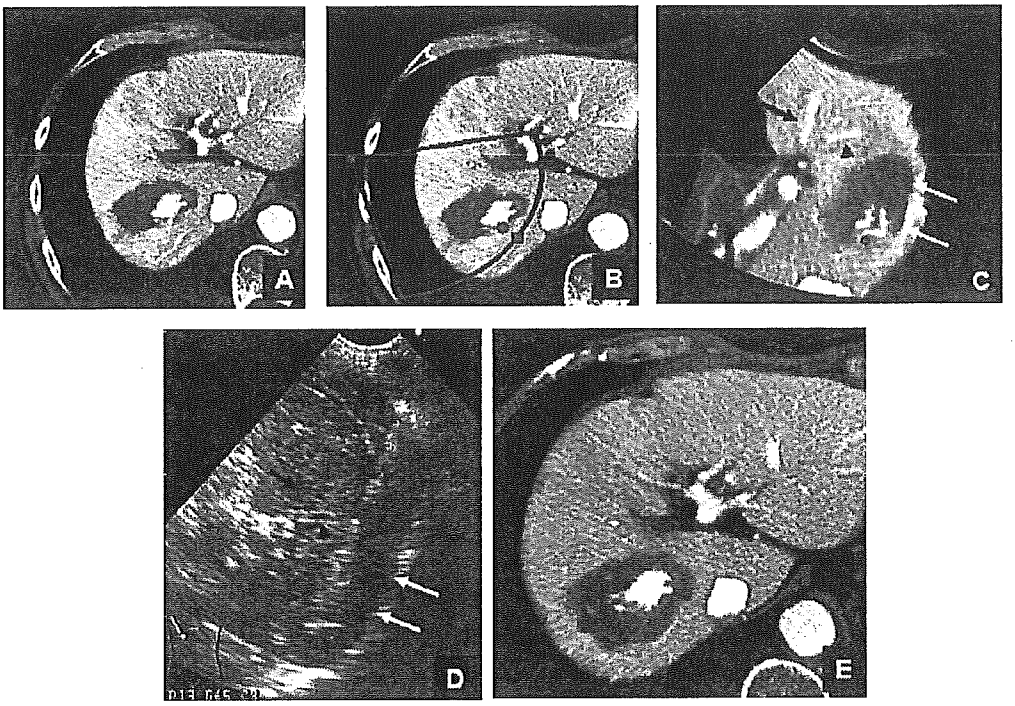

Fig. 5. Treatment of hepatocellular carcinoma using virtual imaging. (A) Dynamic CT showing incomplete necrosis. (B) A gray point is placed on the target site. (C) The virtual image including the gray point is revealed. Anterior branches of portal vein (black arrow and arrowhead) and the necrotic area from previous RFA (white arrow) are shown. (D) Comparison of the image from (C) on conventional US. (E) After treatment, dynamic CT reveals a complete necrotic area.

[15–17]. As post-RFA lesions display a very irregular area and target lesions can be difficult to identify, treatment is often complicated by the need for additional sessions after the initial session of RFA. Treatment of such lesions can reportedly be performed using contrast enhanced US [18–20]. However, this method is very difficult and not all lesions are contrasted. In such cases, virtual US facilitates treatment after previous RFA.

In conclusion, virtual US is might be useful for visualization of HCC nodules that those cannot be seen by conventional US. Thus, virtual US greatly assists US-guided treatment for HCC.

Acknowledgements

We wish to express our thanks to Shogo Azemoto and Masumoto Shun (Medical Imaging Laboratory) for their cooperation in the development of this software and to Teruhito Mochizuki, Seishi Kumano, and Toyoaki Haraikawa (Department of Radiology, Ehime University School of Medicine) for their cooperation.

References

[1] Hu H. Multi-slice helical CT: scan and reconstruction. Med Phys 1999;26:5–18.
[2] Taguchi K, Aradate H. Algorithm for image reconstruction in multi-slice helical CT. Med Phys 1998;25:550–61.
[3] Fuchs T, Kachelriess M, Kalender WA. Technical advances in multi-slice spiral CT. Eur J Radiol 2000;36:69–73.
[4] Weidenbach M, Wick C, Pieper S, et al. Augmented reality simulator for training in two-dimensional echocardiography. Comput Biochem Res 2000;33:11–22.
[5] Fenlon HM, Nunes DP, Schroy PC, et al. A comparison of virtual and conventional colonoscopy for the detection of colorectal polyps. N Engl J Med 1999;341:1496–503.
[6] Vining DJ. Virtual colonoscopy. Semin Ultrasound CT MR 1999;20:56–60.
[7] Nico B, Charles L, Jos RTCR, et al. Three-dimensional echocardiography paves the way toward virtual reality. Ultrasound Med Biol 2000;26:1065–74.
[8] Hans-Heino E. SONOSim3D: a multimedia system for sonography simulation and education with an extensible case database. Eur J Ultrasound 1998;7:225–30.
[9] Dong B, Liang P, Yu X, et al. Percutaneous sonographically guided microwave coagulation therapy for hepatocellular carcinoma: results in 234 patients. Am J Roentgenol 2003;180:1547–55.
[10] Shiina S, Yasuda H, Muto H, et al. Percutaneous ethanol injection in the treatment of liver neoplasms. Am J Roentgenol 1987;149:949–52.
[11] Solmi L, Muratori R, Bertoni F, et al. Echo-guided percutaneous ethanol injection in small hepatocellular carcinoma: personal experience. Hepatogastroenterology 1993;40:505–8.
[12] Francica G, Marone G. Ultrasound-guided percutaneous treatment of hepatocellular carcinoma by radio frequency hyperthermia with a 'cooled-tip needle'. A preliminary clinical experience. Eur J Ultrasound 1999;9:145–53.
[13] Giorgio A, Tarantino L, de Stefano G, et al. Percutaneous sonographically guided saline-enhanced radiofrequency ablation of hepatocellular carcinoma. Am J Roentgenol 2003;181:479–84.